2015 IEEE 12th International Conference on Mobile Ad Hoc and Sensor Systems

Interference Cancellation in Multiuser Acoustic Underwater Networks Using Probabilistic SDMA

Mehdi Rahmati and Dario Pompili
Dept. of Electrical and Computer Engineering, Rutgers University–New Brunswick, NJ, USA
E-mails: {mehdi_rahmati, pompili}@cac.rutgers.edu

***Abstract*—Combating interference is an important yet challenging issue for multiuser communications especially in the harsh underwater acoustic environment. In this paper, a novel Angle-Of-Departure(AOD)-based technique is proposed, which accounts for the inherent position uncertainty of underwater propeller-driven Autonomous Underwater Vehicles (AUVs) or buoyancy-driven gliders. A new probabilistic Space Division Multiple Access (SDMA) technique is studied using confidence interval estimation, and an effective approach to manage interference statistically is discussed. Also, an optimization problem is proposed to mitigate multiuser interference while keeping the transmitter antennae beamwidth at a desirable value so to find a tradeoff among (i) spreading the beam towards the receiver to combat position uncertainty, (ii) focusing such beam to minimize dispersion, and (iii) minimizing interference to other vehicles in the surrounding. Solutions and algorithms are proposed to overcome the multiuser interference via a hybrid SDMA-Time Division Multiple Access (TDMA) method. Simulation results show that the solution mitigates statistical interference, lessens packet retransmission rate, and obtains Signal-to-Interference-plus-Noise Ratio (SINR) gain and rate efficiency over conventional TDMA and SDMA methods.**

***Index Terms*—Interference Cancellation; Medium Access Control; Probabilistic SDMA; Underwater Acoustic Networks.**

I. Introduction

Over the past few years, underwater communications and networks comprising static sensors as well as mobile vehicles have attracted the attention of researchers and engineers due to the wide and various range of the applications enabled. Oceanographic data collection, pollution monitoring, offshore exploration, disaster prevention, assisted navigation, and tactical surveillance are just some of these applications [1]. Underwater wireless communications based on acoustic waves with respect to radio frequency waves suffer from (i) more limited bandwidth, lower bound by environment noise and upper bound by transmission loss due to spreading and absorption; (ii) higher propagation delay; (iii) higher bit error rate; and (iv) unreliable and time-varying channel. Besides, the acoustic wave speed is not constant and depends on temperature, salinity, and pressure of the body of water traversed [2].

Recently, Multiple Input Multiple Output (MIMO) antenna techniques have been investigated and showed to be very promising in achieving high speed communications. However, in a multiuser scenario, the interference probability rises and the overall performance will be considerably impacted. This problem is addressed in designing a Medium Access Control (MAC) protocol, which aims at sharing *fairly* and *efficiently* the common medium resource among active transmitters, whereas many existing terrestrial techniques are not reliable solutions for underwater acoustic networks [1].

A. Motivation

One promising yet unexplored underwater MAC technique exploits the spatial separation of the users. This technique is called Spatial Division Multiple Access (SDMA) and makes use of the fact that users are not located simultaneously in the same location or that at least such event has very low probability [3]. This assumption is very realistic in interference cancellation applications when the number of nodes is low. As vehicles and sensors are usually deployed very sparsely underwater, SDMA represents potentially a very interesting MAC approach for such an environment.

However, the conventional terrestrial SDMA approach is not appropriate for underwater applications. There are many reasons to question the reliability of this method since the underwater channel state information is unknown to both transmitter and receiver; also, finding a reliable channel estimation is challenging due to the fast-varying characteristic of underwater channels. Furthermore, implementing SDMA requires the position information of each underwater vehicle, which is not easily available as the Global Positioning System (GPS) does not work underwater. Considering the effect of ocean currents on the vehicles, inaccuracies in position estimation increases their position uncertainty [4] and this leads to performance degradation of SDMA. This uncertainty becomes worse over time when the vehicle stays more underwater, which leads to non-negligible drifts in the the vehicle's position, thus making traditional SDMA useless. One solution could be adding a localization technique [5] along with SDMA, but this would bring more complexities and challenges.

B. Related Work

Multiuser interference has always been a challenge underwater. In [6], the region of feasibility has been considered for interference alignment in underwater MIMO sensor networks. Code Division Multiple Access (CDMA) as a promising underwater MAC has been investigated in the literature [7], [8]. In [9], the proposed MAC protocol uses time frames (TDMA), which is efficient in terms of interference cancellation but increases packet delay and latency in the network. The authors in [3] argued that SDMA in Radio Frequency (RF) channels can minimize the multiuser interference. An overview of the

978-1-4673-9101-6/15 $31.00 © 2015 IEEE
DOI 10.1109/MASS.2015.101

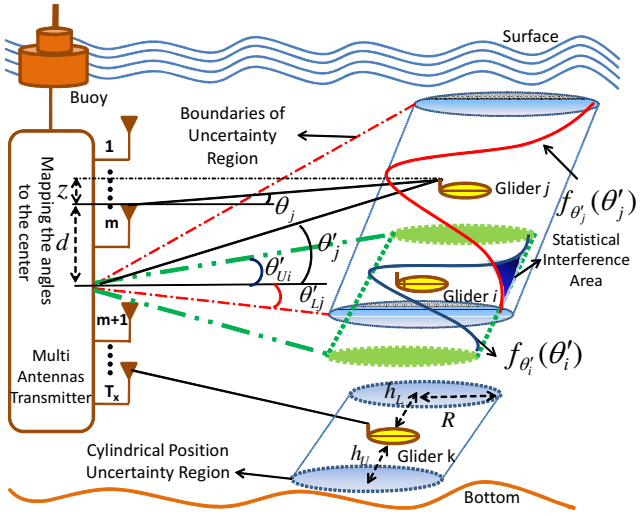

Fig. 1. Vertical view of the system model representing gliders j and i overlap leading, as a result, to statistical acoustic interference. Position uncertainty regions and the distribution of the gliders are shown. To unify the coordinates, angles are mapped from the top of the antennae to the center point.

basic principles for applying smart antenna to SDMA in mobile networks is provided in [10], where it is shown how SDMA can increase cellular network capacity.

Furthermore, since SDMA should separate the users in spatial domain, opportunistic beamforming approaches have been investigated for SDMA in radio communications. In [11], beamforming schemes are proposed for multiuser MIMO-SDMA downlink systems. In [12], a robust/self-organizing SDMA approach is proposed in which the geographical locations of the users are divided into smaller spaces. The main issue in this context is the inaccuracy and uncertainty in the user location. Considering the effect of ocean currents on the location of the underwater vehicles, inaccuracies in position estimation get worse and increase the position uncertainty of underwater vehicles, which leads to performance degradation. In [4], an approach has been proposed to predict gliders' position as well as their region of confidence.

C. Contribution

Interference mitigation via a *deterministic* approach is not an efficient solution to the above problem as it ignores the inherent position uncertainty of the vehicles caused by drifts, model errors, not up-to-date neighboring discovery information, thus leading to performance degradation.

In this paper, we propose a novel *statistical/probabilistic* interference-cancellation method for multiuser multiple-antenna underwater acoustic networks. Our method, called *probabilistic SDMA*, separates the gliders in the 3D space by integrating a statistical approach and a position-uncertainty estimation technique. We exploit interval estimation to calculate the spatial position of the users and to determine the beam characteristics of each antenna in a MIMO array antenna structure. We cast an optimization problem to mitigate the interference while keeping the transmit beamwidth within a desirable range so to find a tradeoff among (i) spreading the beam towards the receiver to combat position uncertainty, (ii) focusing such beam to minimize dispersion, and (iii) minimizing interference to other vehicles with high confidence.

Furthermore, in the case when the gliders' uncertainty regions are entirely overlapped such that they cannot be separated via the optimization problem and pure SDMA, we propose a novel hybrid probabilistic SDMA-TDMA MAC protocol that leads to a reliable and collision-free MAC technique. We will show that this method outperforms conventional TDMA in terms of *rate efficiency* and *SINR*. We also introduce a new definition for *retransmission rate* to evaluate the performance of our proposed method in different situations, before and after performing optimization problem.

The remainder of this paper is organized as follows. In Sect. II, we review the system model; in Sect. III, we introduce the proposed system and provide solutions for a hybrid SDMA-TDMA MAC. In Sect. IV, we present the simulation results and discuss the benefits of our solution. Finally, in Sect. V, we draw the main conclusions.

II. System Model

Figure 1 illustrates the proposed 3D system model in which a Multiple Input Single Output (MISO) array antenna is considered in a downlink transmission from an ocean buoy, as the transmitter, to gliders, as receivers. As discussed in [4], assuming that ocean currents are unknown, the glider's drifting in the horizontal plane is identically and independently distributed (i.i.d.) and follows a normal distribution, which makes the horizontal projection of its confidence a circular region. Regarding the glider's movement along its trajectory, the uncertainty region is concluded to be a cylinder.

Since the uncertainty regions of gliders j and i overlap, as shown in Fig. 1, we can imagine that a high probability of interference occurs between them. Assume the angles of departure, corresponding to each pair of gliders, are identified as θ_j and θ_i, and mapped from the m^{th} and $(m+1)^{th}$ antennae, $\forall m \in 1, ..., (T_x - 1)$, to their center point to unify the coordinates, where T_x is the total number of antennae at the transmitter and ${\theta_j}'$ and ${\theta_i}'$ are the transferred angles corresponding to gliders j and i. We can conclude that $\tan({\theta_j}') = (1 + \frac{d_m}{z_{jm}})\tan(\theta_j)$, where z_{jm} is the vertical distance between the depth of glider j and antenna m, and d_m is the distance between the center point and antenna m. In the case where z_{jm} is much greater than d_m, ${\theta_j}' \approx \theta_j$. Figure 2 displays the beam specifications as well as its projections on the vertical(θ) and horizontal(ϕ) planes. All angles are mapped into a single point, thus, in the horizontal plane, we have ${\phi_j}' = \phi_j$.

In this paper, we focus on the effect of direct line of sight beam interference cancellation. We assume the transmission occurs at short distances in which the direct beam is strong and dominant enough over the reflected beams from the surface and the bottom of the sea. In this case, the acoustic waves propagate in a straight line and the propagation delay is small. For farther distances (above tens of kilometers),

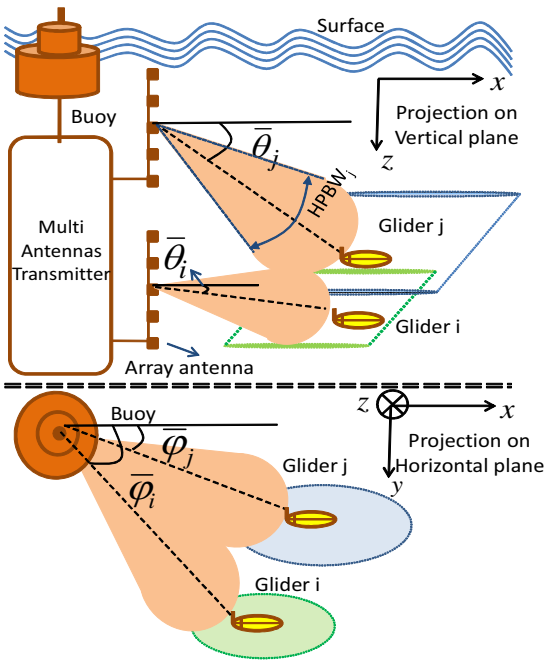

Fig. 2. Vertical and horizontal cut-views along with the antenna pattern radiation in the vertical (θ) (top) and horizontal (ϕ) (bottom) planes. Antenna arrays are used to form the beam along a desired direction.

depending on the sound profile, the acoustic rays bend towards the region of lower acoustic speed (the so-called *"laziness law"*). This effect, as a result, changes the angles and the estimations. Long and variable propagation delays lead to a bottleneck in the time synchronization. Obviously, short-distance communication is also useful for applications where power consumption is a challenge as via multi-hopping, i.e., using multiple shorter communication links and intermediate relay nodes, the transmitter's output power can be decreased via power control, thus saving energy and increasing battery lifetime. Here, we use the underwater pathloss model described in [2] as $A(l,f) = A_0 l^k a(f)^l$, where f [KHz] denotes frequency, l [Km] is the distance, A_0 is a scaling factor, and $a(f)$ represents the absorption coefficient, which is obtained, in dB/km, as $0.11\frac{f^2}{1+f^2}+44\frac{f^2}{4100+f^2}+2.75\times10^{-4}f^2+0.003$. The channel transfer function is therefore $H(l,f)=\frac{1}{\sqrt{A(l,f)}}$.

III. Our Solution

We present here our approach and discuss its applicability to dual- and multi-glider scenarios. First, in Sect. III-A, we introduce the theory of estimating the required values for AOD and beamwidth of each antenna in a dual-glider mission. The proposed probabilistic SDMA concept is introduced and our statistical interference cancelation optimization problem along with the associated algorithm are discussed. Also, a new metric – called probabilistic retransmission rate – is defined to calculate the risk of the proposed method. Then, in Sect. III-B, we consider the problem in a more dense situation with multiple gliders where SDMA alone would underperform and propose a hybrid probabilistic SDMA-TDMA MAC protocol.

A. Interference Cancellation for a Dual-Glider Mission

1) Confidence Interval Estimation: Since variation of glider's position inside the cylinder can be defined as a normal random variable (r.v.) [4], it is inferred that the variation of the angles at the transmitter side is also a normal r.v. with unknown mean and variance. Also, we claim that each sample of angle is a result of the glider's drift as $\theta_n = \tan^{-1}(z_n/x_n)$. Hence, based on Taylor's polynomial approximation, $\tan^{-1}(z_n/x_n) \approx z_n/x_n - 1/3(z_n/x_n)^3 + 1/5(z_n/x_n)^5 - ...$, where z_n is the glider's vertical drift due to its position uncertainty and is very small in comparison with x_n, which is the horizontal distance between the glider and the transmitter; consequently, $\theta_n \approx z_n/x_n$. Besides, [13] provides approximations that demonstrate in practice that many of the ratios of normal r.v. are normally distributed. Based on the numerical calculations in [13], z_n/x_n and so θ_n have normal distributions.

Statement 1: Since θ_n's are random samples of a normal distribution, $\mathcal{N}(\mu,\sigma^2)$, recalling from the statistical inference theorem [14], $\bar{\theta}$ and $(S^{(\theta)})^2$ are also independent r.v.'s and $\bar{\theta}$ has a normal distribution, $\mathcal{N}(\mu,\sigma^2/2)$. Besides, $\frac{\bar{\theta}-\mu}{S^{(\theta)}/\sqrt{n}}$ has a student's t-distribution with $n-1$ degrees of freedom.

Definition 1: An interval estimate of a parameter Γ is any pair of $L(X)$ and $U(X)$ for which, by observing $X=x$, it is inferred that $L(X)\le\Gamma\le U(X)$. This interval, together with $P(\Gamma\epsilon\,[L(X),U(X)])$, is called confidence interval [14].

Definition 2: A r.v. $Q(X_1,...,X_n,\Gamma)$ is called a pivotal quantity if its distribution is independent of all parameters Γ.

Statement 2: It is demonstrated in [14] that for pivotal quantity $Q(X,\Gamma)$, confidence interval for any parameter Γ can be defined as $P_\Gamma(a\le Q(X,\Gamma)\le b)\ge 1-\alpha$, and $C(X)=\{\Gamma_0 : a\le Q(X,\Gamma_0)\le b)\}$, where Γ_0 is one of the parameter sets of Γ and $C(X)$ is its $1-\alpha$ confidence degree.

Considering Definition 2 and Statement 1, it is inferred that $\frac{\bar{\theta}-\mu}{S^{(\theta)}/\sqrt{n}}$ is a pivot since the t-distribution does not depend on μ,σ^2. Using Statement 2, we calculate the confidence interval for the mean of θ of each glider as,

$$P(\theta_{Lj}\le\mu_{\theta_j}\le\theta_{U_j})\ge 1-\alpha, \tag{1}$$

$$\theta_{Lj}=\bar{\theta_j}-t_{N-1,\alpha/2}\frac{S^{(\theta_j)}}{\sqrt{N}},$$

$$\theta_{Uj}=\bar{\theta_j}+t_{N-1,\alpha/2}\frac{S^{(\theta_j)}}{\sqrt{N}}, \tag{2}$$

where θ_{Lj} and θ_{Uj} are interval boundaries, and $\bar{\theta_j}$ and $S^{(\theta_j)}$ are estimation of the mean and standard deviation, respectively, and can be derived as,

$$\bar{\theta_j}=\sum_{n=1}^{N}\frac{\theta_{jn}}{N}, \tag{3}$$

$$S^{(\theta_j)}=\left[\frac{1}{N-1}\sum_{n=1}^{N}\left(\theta_{jn}-\bar{\theta_j}\right)^2\right]^{\frac{1}{2}}. \tag{4}$$

With reference to Fig. 2, similar calculations will be done for ϕ in the horizontal plane; since the radiated pattern has a 3D structure, both $\bar{\theta}_j$ and $\bar{\phi}_j$ should be estimated.

2) Probabilistic SDMA Concept: In our solution, the transmitter should be able to adjust its beam's direction towards each glider and modify its beamwidth within a confident range to cover the desired user. Beam's direction in the vertical and horizontal planes are defined as $\bar{\theta}_j$ and $\bar{\phi}_j$, respectively, and the beamwidth is assumed homogeneous in both planes. The beamwidth is chosen in such a way that it is equal to the confidence interval of $\bar{\theta}_j$. In other words, the transmitter forms the beam in an interval of $\pm t_{N-1,\alpha/2}\frac{S^{(\theta_j)}}{\sqrt{N}}$ around $\bar{\theta}_j$, i.e.,

$$AOD_j^{\theta} = \bar{\theta}_j, \quad AOD_j^{\phi} = \bar{\phi}_j, \quad HPBW_j = \theta_{U_j} - \theta_{L_j}, \quad (5)$$

where AOD_j^{θ} and AOD_j^{ϕ} are the angles of departure in the vertical and horizontal directions towards glider j, and $HPBW_j$ is the related Half Power Beam Width for glider j. A reliable method to control the beam's direction is using *arrays of antennae*. The angular pattern specifications, i.e., its AOD and beamwidth, define the number, geometrical arrangement, and relative amplitudes and phases of the array elements [15].

3) Statistical Interference Cancellation: By knowing the probability distributions of the gliders' position, we estimate the probability of interference by defining the *statistical interference*. We cast an optimization problem whose objective function $\mathcal{F}$ is to minimize this interference, i.e., to find the maximum HPBW for all interfering gliders while satisfying the minimum interference requirements, i.e.,

Given: $HPBW_{thr}, HPBW_j, HPBW_i, \theta'_{Uj}, \theta'_{Li}, P_{Ithr}$,
Find: $(\bar{\theta}'_j)^*, (\bar{\theta}'_i)^*, (S^{\theta'_j})^*, (S^{\theta'_i})^*$,

$$\textbf{Min} \quad \mathcal{F} = \frac{\sqrt{(S^{(\theta'_j)})^2 + (S^{(\theta'_i)})^2}}{\bar{\theta}'_j - \bar{\theta}'_i}; \quad (6)$$

$$\textbf{S.t.:} \quad HPBW_{thr} < 2(t_{N-1,\alpha/2}\frac{S^{(\theta'_j)}}{\sqrt{N}}) < HPBW_j, \quad (7)$$

$$HPBW_{thr} < 2(t_{N-1,\alpha/2}\frac{S^{(\theta'_i)}}{\sqrt{N}}) < HPBW_i, \quad (8)$$

$$\bar{\theta'}_j + (t_{N-1,\alpha/2}\frac{S^{(\theta'_j)}}{\sqrt{N}}) < \theta'_{Uj}, \quad (9)$$

$$\bar{\theta'}_i - (t_{N-1,\alpha/2}\frac{S^{(\theta'_i)}}{\sqrt{N}}) > \theta'_{L_i}, \quad (10)$$

$$\bar{\theta'}_i + (t_{N-1,\alpha/2}\frac{S^{(\theta'_i)}}{\sqrt{N}}) \geq \bar{\theta'}_j - (t_{N-1,\alpha/2}\frac{S^{(\theta'_j)}}{\sqrt{N}}), \quad (11)$$

$$P_I(i,j) \leq P_{Ithr}. \quad (12)$$

The overlapping interference area in (6) will be minimized if its denominator increases or its numerator falls, which, in turn, means reducing $S^{(\theta'_j)}$ and $S^{(\theta'_i)}$. Moreover, HPBW directly depends on the standard deviation. Thus, reducing $S^{(\theta'_j)}$ and $S^{(\theta'_i)}$ lessens HPBW of both gliders and decreases the interference probability. Consequently, in (7)-(8), we keep the new beamwidth higher than a threshold value and smaller than the cylinder size, i.e., the old HPBW.

Optimal values should be computed such that the beam areas do not exceed the uncertainty region. The conditions in (9)-(10) keep the new boundaries of gliders j and i inside the uncertainty areas. With (11), we prevent the beams to become very narrow, since it is sufficient to keep the interference probability less than a threshold value of P_{Ithr} as in (12), where $P_I(i,j)$ is the probability of interference between the two gliders. Note that in the case of interference, the upper boundary of the confidence interval for glider i passes the lower boundary of the interval for glider j. Inspired by the *stress-strength interference theory* [16], since θ'_j and θ'_i are normal r.v.'s with means of $\bar{\theta}'_j$, $\bar{\theta}'_i$ and standard deviations of $S^{(\theta'_j)}$, $S^{(\theta'_i)}$, we define $f_{\theta'_I}(\theta'_I)$ as the probability distribution function of the interference, which is also a normal distribution with mean of $\bar{\theta}'_j - \bar{\theta}'_i$ and standard deviation of $\sqrt{(S^{(\theta'_j)})^2 + (S^{(\theta'_i)})^2}$.

Therefore, $P_I(i,j)$ can be calculated as,

$$P_I(i,j) = P(\theta'_{U_i} > \theta'_{L_j}) = P(\theta'_{U_i} - \theta'_{L_j} > 0)$$
$$= \int_{IA} f_{\theta'_I}(\theta'_I)d\theta'_I, \quad (13)$$

where IA stands for the *interference area*. We will solve the optimization problem numerically for different angles and locations in Sect. IV based on the theory in [17].

4) Probabilistic Retransmission Rate: As discussed earlier, when the beamwidth becomes very small or the beams are placed far from each other, the probability of interference is minimal. On the other hand, it is possible that the gliders go out of their transmission coverage and probabilistically be 'out of range'. In this case, we would need to retransmit the lost packets, which would result in decreasing the net data rate. In other words, to control the efficient rate, we should avoid retransmission due to a failure or disconnectivity, where the former is the result of interference and the latter is the consequence of missing the target. We define *retransmission rate* as a measure of the system's need to resend packets. Prior to performing our interference cancellation method, this metric is defined as $r_{reT,j}^{pre} = \frac{P_I(j,i)}{P_{success,j}}$. Probability of successful transmission is the probability of using a beam with a width equal to the uncertainty region without interfering with any other beams, and we define it as,

$$P_{success,j} = \int_{\theta'_{Lj}}^{\theta'_{Uj}} f_{\theta'_j}(\theta'_j)d\theta'_j. \quad (14)$$

After interference cancellation, we define the *retransmission rate* as $r_{reT,j}^{post} = \frac{P_{retran,j}}{P_{success,j}}$, where $P_{retran,j}$ is the probability that a glider falls out of the coverage of the transmitter, and we define it as,

$$P_{retran,j} = \int_{\theta'_{Lj}}^{(\bar{\theta'}_j)^* - \frac{(HPBW_j)^*}{2}} f_{\theta'_j}(\theta'_j)d\theta'_j$$

$$+\int_{(\bar{\theta'}_j)^*+\frac{(HPBW_j)^*}{2}}^{\theta'_{Uj}} f_{\theta'_j}(\theta'_j)d\theta'_j. \quad (15)$$

5) AOD and Beamwidth Estimation Algorithm: First, we define a protocol for interference mitigation between two gliders; then, we introduce three scenarios for multiple users; finally, we present a general MAC method. Algorithm 1 looks for an estimation of the AOD and HPBW; it starts by estimating the angles, their statistical parameters, and confidence interval boundaries. By comparing the upper boundary of glider $j+1$ with the lower boundary of glider j in both the vertical and horizontal planes, it checks the existence of overlap. If case of detecting interference in both planes, the algorithm goes through the interference cancellation step. Solving the optimization problem is meaningful *iff* $\theta'_{U,j+1} > \theta'_{L,j}$ *and* $\theta'_{L,j+1} < \theta'_{L,j}$. The latter condition ensures that the second glider is not completely inside the uncertainty region of the first glider, which would result in an entire overlap. We define such situation as *failure switch*, which would trigger the algorithm to cluster the strong interfered gliders in a different team. This concept will be discussed in the next section.

Algorithm 1 AOD and Beamwidth Estimation

Input:$[location_j(n); n = 1 : N]$
Output:AOD and beamwidth, Failure Switch
  for every two neighboring gliders **do**
    Calculate angles (θ_{jn}, ϕ_{jn}); Calculate statistical parameters (θ_j, θ'_j, ϕ_j, ϕ'_j)
  end for
  Failure Switch $\leftarrow$ 0
  if ($\theta'_{U,j+1} < \theta'_{L,j}$ OR $\phi'_{U,j+1} < \phi'_{L,j}$) **then**
    Calculate AODBeam (AOD_j, AOD_{j+1}, $HPBW_j$, and $HPBW_{j+1}$)
  else
    if $\theta'_{L,j+1} < \theta'_{L,j}$ **then**
      Run optimization problem considering the constraints
      if problem returns optimum values: $(\bar{\theta}'_j)^*$, $(\bar{\theta}'_{j+1})^*$, $(S^{\theta'_j})^*$, $(S^{\theta'_{j+1}})^*$ **then**
        Calculate AODBeam (AOD_j, AOD_{j+1}, $HPBW_j$, and $HPBW_{j+1}$, optimum values)
      else
        Failure Switch $\leftarrow$ 1
      end if
    else
      Failure Switch $\leftarrow$ 1
    end if
  end if

B. Interference Cancellation for a Multiple-Glider Mission

In an underwater environment with N gliders, assume each transmitter antenna tracks one or more glider, in a sequential manner, based on the depth of the users in the water. Depending on the vehicles' relative positions, several scenarios can be considered. The difference between the proposed scenarios is the limitation of using SDMA when some gliders are overlapped more than expected. Thus, if a space separation cannot be implemented using Algorithm 1, we propose a new hybrid probabilistic SDMA-TDMA MAC method that leads to a collision-free underwater multiple access protocol suitable for time-insensitive applications.

1) Scenario I, Pure SDMA (best case): In this scenario, SDMA can be implemented completely and the number of gliders is equal to the number of transmitter antennae. Deployment is such that each glider can be tracked by its corresponding antenna. Gliders can be either separable in at least one of two planes or the optimization problem is able to separate them. In other words, in this case failure switch in Algorithm 1 never returns 1. The transmitter communicates with all the gliders simultaneously; hence, only one time slot is needed. Obviously, rate efficiency has the best value among all other possible scenarios.

Algorithm 2 SDMA with Intra-Cluster TDMA

Input: N: number of gliders
Output: clusters(CL), time slots(M), number of clusters(k)
  M $\leftarrow$ 1; $k \leftarrow$ 1; //default number of time slots and clusters
  for all gliders **do**
    Call Algorithm 1 (gliders j,j+1)
    if Failure Switch==1 **then**
      CL(k) $\leftarrow$ (glider j and glider j+1); //put both gliders in a single cluster.
    else
      CL(k) $\leftarrow$ glider j and CL(k+1) $\leftarrow$ glider j+1; //put gliders in different clusters.
      k=k+1; //counting the number of clusters.
    end if
  end for
  M $\leftarrow$ max(size(CL)); //max number of gliders in a single cluster.

2) Scenario II, SDMA with Intra-Cluster TDMA: Similarly to Scenario I, assume the number of gliders is always less than or equal to the number of antennae. It is possible that interference occurs in a way that the beam separation could not be performed in any of the two planes. The failure switch in Algorithm 1 might return 1 in some circumstances. Therefore, we have to cluster the non-separable gliders and perform SDMA for clusters, instead of individual gliders. For the clusters containing more than one glider, time-domain sharing is also performed, so we have an Intra-Cluster TDMA in addition to SDMA. Algorithm 2 calculates the content of each cluster, the number of clusters, and time slots.

Algorithm 3 SDMA with Inter-Cluster TDMA

Input: N: number of gliders, Tx: Number of transmitter antennae
Output: clusters(CL), time slots(M_1,M_2), number of clusters(k)
  $M_1 \leftarrow 1$; $M_2 \leftarrow 1$; $k \leftarrow 1$; //default number of time slots and clusters.
  Call Algorithm 2 ( ); $M_1 \leftarrow$ return Algorithm 2 ( )
  if $k > Tx$ **then**
    External clustering ( ) AND Inter-Cluster TDMA ( ): do until $k \leq$Tx
    for $p = 1 : k-1$ // for all clusters **do**
      scl(p)=(size(CL(p))+size(CL(p+1)));//cluster size for each pair of gliders.
    end for
    External clustering (clusters with $M_3 = min(scl)$); $M_2 = k - Tx + 1$;
  else
    $M_2 = 1$; // There is no external clustering.
  end if

3) Scenario III, SDMA with Inter-Cluster TDMA: As in Fig. 3, assume the number of gliders to be greater than the number of transmitter antennae. Each cluster contains neighboring gliders that are non-separable and so their corresponding failure switches are active per Algorithm 1. If the number of clusters is more than the number of antennae, an additional clustering is required, which leads to form an Inter-Cluster TDMA frame. Algorithm 3 calculates the content of each cluster (CL), the number of clusters (k), and the required time slots and frames (M_1, M_2). This clustering is performed in such a way that the total number of time slots is minimized.

4) Hybrid SDMA-TDMA Multiple Access Protocol: Figure 4 represents the flowchart of the proposed solution. After

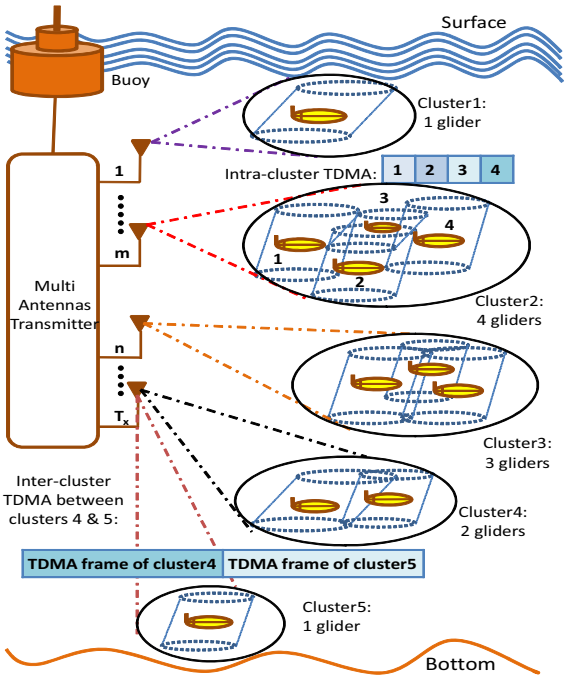

Fig. 3. Example case for Scenario III with different numbers of gliders in each cluster. As the gliders are more than the transmitter antennae, an additional clustering is required and an Inter-Cluster TDMA frame is used.

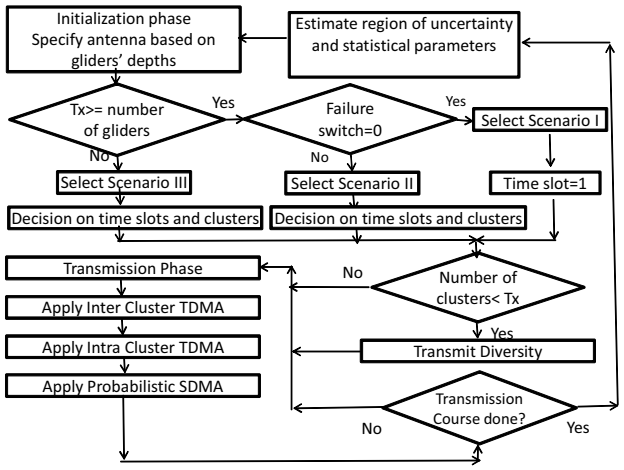

Fig. 4. Flowchart of the proposed hybrid SDMA-TDMA technique.

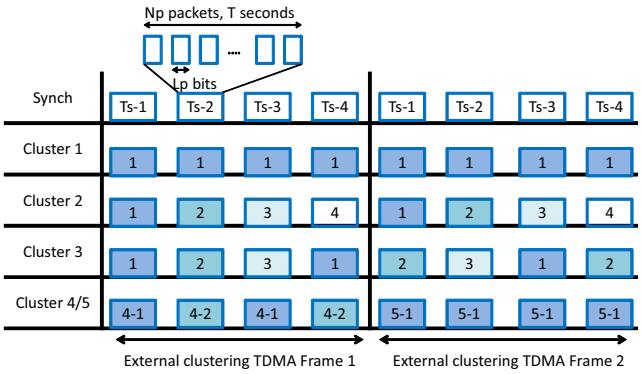

Fig. 5. Timing and synchronization diagram at the transmitter side for the example in Fig. 3. Note that the number in each time slot stands for the ID of the glider that is currently using the channel in each cluster.

estimating the position uncertainty and statistical parameters, the transmitter chooses a scenario based on the number of gliders/transmitter antennae and also on the output of the optimization problem. The appropriate algorithm performs the clustering and calculates the number of time slots for the chosen scenario. When the number of clusters is less than the number of transmitter antennae, we perform a transmit diversity method to use all the resources efficiently. In transmit diversity, the signal propagates from two or more antennae to a single glider, which leads to a diversity gain if the links are independent. This problem will be addressed in our future work. In this paper, we assume the number of clusters is more than or equal to the number of antennae.

Figure 5 represents the time synchronization diagram at the transmitter considering the case study observed in Fig. 3. The number written in each time slot stands for the ID of the glider that is currently using the channel in each cluster. Although underwater acoustic networks suffer from long and variable propagation delay, as we assume short-range communications, the propagation delays can be neglected. We define *time slot usage ratio* for SDMA-TDMA approach as,

$$r^{cl}_{Ts,SDMA-TDMA} = \frac{n^{cl}_{Ts}}{M_2 \max(M_1, M_3)}, \qquad (16)$$

where n^{cl}_{Ts} is the total number of time slots dedicated to each glider of cluster cl in M_2 frames. The denominator is the total number of time slots. The time slot usage ratio for conventional TDMA is calculated as $r_{Ts,TDMA} = \frac{1}{M_{TDMA}}$, in which M_{TDMA} is the total number of time slots, which is equal to the number of gliders. We define *rate efficiency* of the proposed hybrid SDMA-TDMA technique to traditional TDMA as $\eta_{T-S} = \frac{r^{cl}_{Ts,SDMA-TDMA}}{r_{Ts,TDMA}}$.

The effective data rate per user over the total transmission time is defined in [18] as $\frac{1}{N} B \log_2(1+SNR)$, where N is the number of time slots, B is the channel bandwidth, and SNR is the received Signal-to-Noise Ratio. We calculate the effective data rate of each glider in *one* transmitting frame, for Scenario III in hybrid SDMA-TDMA system as,

$$R^{cl}_{SDMA-TDMA} = \frac{N_p\, L_p\, n^{cl}_{Ts}/M_2}{\max(M_1, M_3)T},$$

$$= \frac{1}{\max(M_1, M_3)} Blog_2(1 + SINR_{SDMA-TDMA}). \qquad (17)$$

In (17), N_p and L_p are number and length of packets, and T is the time duration of each time slot. If we adopt the conventional TDMA, $R_{TDMA} = \frac{N_p L_p}{T M_{TDMA}} = \frac{1}{M_{TDMA}} B \log_2(1 + SINR_{TDMA})$. The SINR gain of our proposed method over

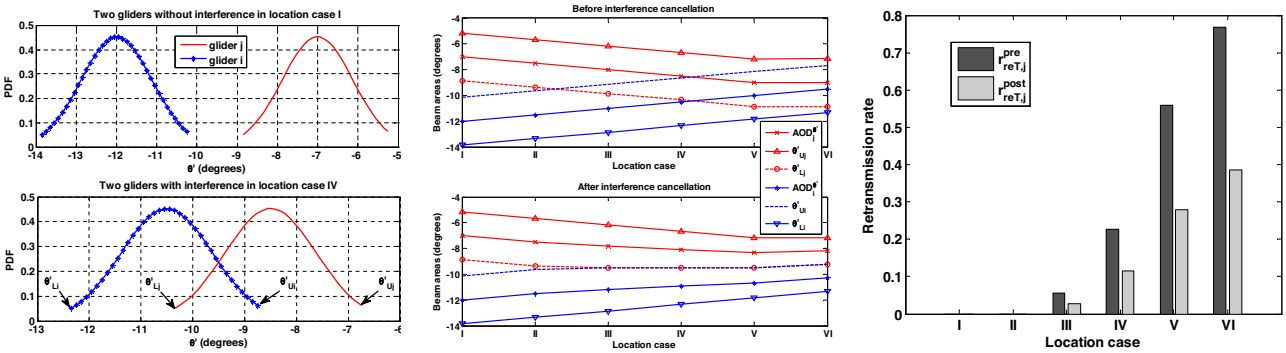

Fig. 6. (a) Probability Density Function (PDF) of AODs for two gliders without/with statistical interference; (b) AOD and the boundaries of region of uncertainty before and after interference cancelation; (c) Retransmission rate before and after interference cancelation between two neighboring gliders.

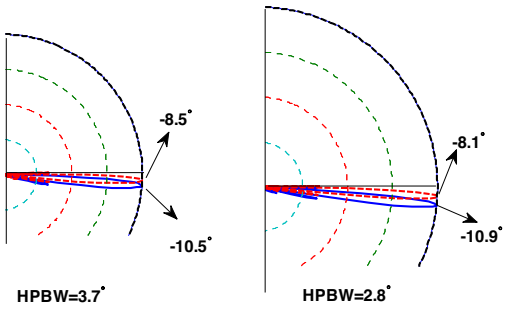

Fig. 7. Patterns of the transmitter arrays for two gliders in angle space before solving the optimization problem (left) and after that (right) for two gliders i and j in location IV.

TDMA is,

$$SINR_{SDMA-TDMA} \approx (SINR_{TDMA})^{\frac{n_{Ts}^{cl}}{M_2}}. \quad (18)$$

IV. Performance Evaluation

Assumptions for the numerical study: We consider a short-range communication system, in which the distance between the transmitter and the users is between 500 m and 1 km. Users are distributed at different depths from the surface to the max depth of 200 m. Let us set the percentage of confidence, i.e., $(1-\alpha)$ in (1), to the common value of 95%. Transmitter uses $N = 20$ samples for estimating the location of each glider. We evaluate our method in six different locations of neighboring gliders, as listed in Table I.

Extracting PDF out of samples: Figure 6(a) shows the PDF's of two neighboring gliders. The top subfigure is the case where the gliders are far away from each other and, hence, do not experience any interference. However, in the bottom subfigure, the overlapping PDFs is evidence of interference (with a certain probability).

Estimating AODs and the boundaries, solving the optimization problem in Scenario I: In Fig. 6(b), we investigate the performance of the proposed optimization problem in Algorithm 1. AODs and uncertainty region boundaries of two gliders are plotted for different locations, before and after performing interference cancellation. At the first and second positions, i.e.. locations I and II, the beam areas of the gliders do not overlap; therefore, the algorithm does not require to run the optimization problem. Conversely, for the other four positions, i.e., locations III to VI, the beam areas penetrate each others, and hence interference occurs. For these situations, the algorithm finds the optimum values for AODs and beam boundaries of gliders. It is apparent in the figure that the optimization problem chooses the largest feasible beamwidths that do not cause any interference.

Evaluating the retransmission rate: As discussed in Sect. III-A4, the probability of interference and of missing the glider, i.e., disconnectivity, lead to the need for retransmission. In Fig. 6(c), we illustrate the retransmission rates, before and after interference cancellation.

TABLE I
Angular Locations of two gliders (in degrees).

Glider ID	I	II	III	IV	V	VI
j	-7	-7.5	-8	-8.5	-9	-9
i	-12	-11.5	-11	-10.5	-10	-9.5

Antenna patterns, all scenarios: Figure 7 shows the patterns of transmitter arrays for gliders j and i, steered towards the corresponding estimated AODs plotted for location IV. In the left subfigure, the interference between the two patterns is apparent; the other subfigure shows the patterns after interference cancellation. It is apparent that the antenna patterns do not have interference anymore. Figure 8(a) illustrates the situation in which two patterns are highly interfered and the optimization problem fails to separate the beams. This might occur in Scenario II or III.

Probabilistic hybrid SDMA-TDMA vs. conventional TDMA, in Scenario III: We consider the example case oin Fig. 3. In Fig. 8(b) we compare the performance of our proposed hybrid SDMA-TDMA method with conventional TDMA, in terms of time slot usage ratio and rate efficiency. Note that the time slot usage ratio for cluster 1, which contains a single glider, is 100%; whereas in TDMA it is 9%, which is a considerable gain. Meanwhile, cluster 5 also has a single

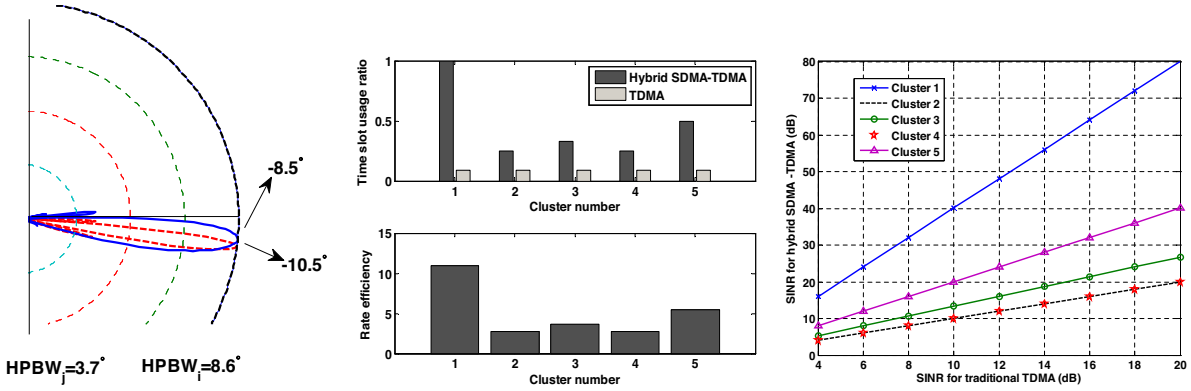

Fig. 8. (a) Pattern of two gliders when their uncertainty regions overlap seriously; (b) Comparison between probabilistic hybrid SDMA-TDMA and conventional TDMA in terms of time slot usage ratio and efficiency for Scenario III and w.r.t. Fig. 3.; (c) SINR gain obtained with hybrid SDMA-TDMA in comparison with conventional TDMA for each cluster for Scenario III and w.r.t. Fig. 3.

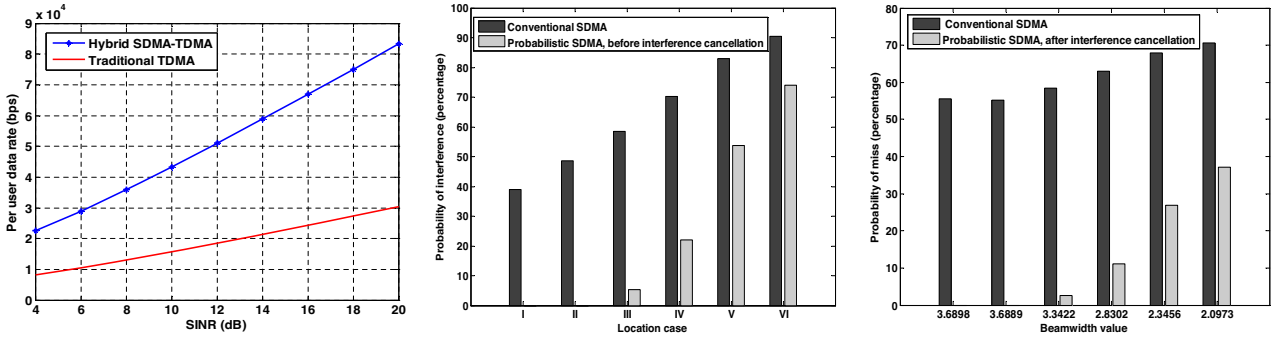

Fig. 9. (a) Comparison between probabilistic hybrid SDMA-TDMA and conventional TDMA in terms of data rate per user; (b) Probability of interference for conventional SDMA and the proposed probabilistic SDMA before interference cancellation; (c) Probability of miss for conventional SDMA and the proposed probabilistic SDMA after interference cancellation.

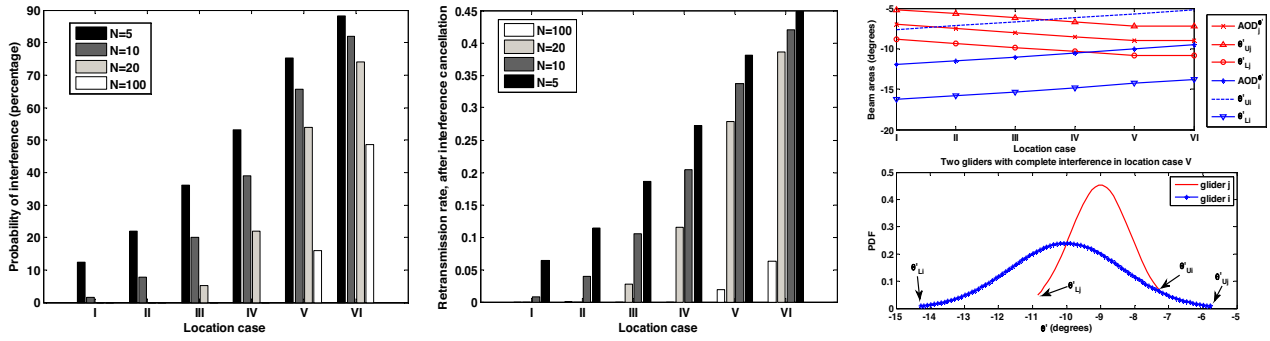

Fig. 10. (a) Probability of interference when different number of samples are exploited; (b) Retransmission rate, after interference cancellation, when using different number of samples; (c) AOD, beam boundaries, and PDF of two interfering gliders that use different number of samples, i.e., $N_j = 20$ and $N_i = 5$.

glider, but since it shares the antenna with cluster 4, its usage ratio is 50%. The rate-efficiency curve confirms that our proposed method outperforms conventional TDMA, for all clusters. Figure 8(c) represents the SINR gain of our proposed method over conventional TDMA. Cluster 1, which contains one glider, has the highest SINR gain among all the clusters. Note that, although cluster 5 has only one member, as it exploits an inter-cluster TDMA with cluster 4, its gain is less than cluster 1. Figure 9(a) compares the hybrid SDMA-TDMA system with traditional TDMA, based on data rate per user, calculated as in (17). This figure shows a considerable gain for our proposed method over conventional TDMA.

Probabilistic SDMA vs. conventional SDMA: In Figure 9(b), probability of interference of the proposed probabilistic SDMA method, before interference cancellation, is compared with a conventional SDMA. In the latter, we assume that the transmitter steers the beam towards every received location, with a constant beamwidth. In order to provide a

fair comparison, suppose its beamwidth is equal to that of the probabilistic SDMA, i.e., 3.7° in all cases. Probability of interference of our method is much less than for conventional SDMA, even before performing optimization. Figure 9(c) displays a comparison between probability of miss of conventional SDMA and probabilistic SDMA, which performs interference cancellation. The horizontal axis shows the value of the beamwidth of the proposed system after optimization. We assume that the conventional SDMA transmits with these beamwidth values. Since it does not utilize any statistical information of the glider's location, it is very likely that it misses the glider. In contrast, probabilistic SDMA might miss the glider with much less probability, and just in those cases when it had to use narrower beam to mitigate interference.

Effect of number of samples (N): Figure 10(a) compares probability of interference when using different values of samples, in all the previously mentioned angular locations. As it is expected, a large N means a more precise estimation and a smaller interval, leading to a narrower beamwidth and so less probability of interference. For the same reason, the probability of miss and thus the retransmission rate after interference cancellation, is lower for larger values of N. This is depicted in Fig. 10(b), which plots this parameter for different values of N. On the other hand, a very large value, like 100 samples, would not be practical since it would impose an big delay to the system. Here, we assume a moderate number of 20 samples, leading to a considerable performance enhancement in comparison with traditional systems. However, $N = 10$ could also be a reasonable choice in some cases, especially when the system is capable to work in an adaptive manner. For instance, let us assume that the gliders are located in location III and the beam parameters are estimated using $N = 10$ samples. For Fig. 10(b), the retransmission rate would be approximately equal to 0.1. If the gliders reach location IV, and still send 10 samples for parameter estimation, the retransmission rate increases to 0.2, which, in turn, leads to decreasing the efficient rate of the system. In this situation, if the gliders sent 10 additional samples, i.e., a total of 20 samples, the retransmission rate would fall again down to 0.1 and thus the efficient rate would increase.

In Fig. 10(c), we investigate the situation when each of the two neighboring gliders uses different number of samples to determine the beam parameters. We assumed $N_j = 20$ for glider j and $N_i = 5$ for glider i. As depicted in the figure, the gliders are interfered from the first location. Moreover, as they move towards each other, the beam of glider j is completely covered by the beam of i from location IV. The PDF's of the two gliders are also plotted to clarify the situation in location V. In these situations, the optimization problem cannot separate the beams and the failure switch in Algorithm 1 would return 1. This would be the case in which the system would perform clustering algorithms and put these two gliders in a single cluster.

V. Conclusion

We proposed a novel statistical interference cancellation method for multiuser underwater acoustic networks and introduced a new position-based probabilistic Space Division Multiple Access (SDMA) technique that employs the interval estimation of the underwater users' position to define the required beam direction and width. We cast and solved an optimization problem to minimize the multiuser interference and compute the corresponding optimum Angle-Of-Departure (AOD) and beamwidth. We also extended this multiple access method to the case of a dense network of underwater vehicles by proposing a hybrid SDMA-Time Division Multiple Access (TDMA) solution. Simulation results showed that the proposed solution minimizes the statistical interference and improves the performance of the system in terms of efficiency and fairness.

Acknowledgment: This work was supported by the NSF CAREER Award No. OCI- 1054234.

References

[1] I. F. Akyildiz, D. Pompili, and T. Melodia, "Underwater Acoustic Sensor Networks: Research Challenges," *Ad Hoc Networks (Elsevier)*, vol. 3, no. 3, pp. 257–279, May 2005.

[2] L. M. Brekhovskikh and I. P. Lysanov, *Fundamentals of ocean acoustics*. Springer, 2003.

[3] C. Ung and R. Johnston, "A space division multiple access receiver," in *Antennas and Propagation Society International Symposium*, vol. 1. IEEE, 2001, pp. 422–425.

[4] B. Chen, P. C. Hickey, and D. Pompili, "Trajectory-aware communication solution for underwater gliders using whoi micro-modems," in *Sensor Mesh and Ad Hoc Communications and Networks (SECON), 2010 7th Annual IEEE Communications Society Conference on*. IEEE, 2010, pp. 1–9.

[5] H.-P. Tan, R. Diamant, W. K. Seah, and M. Waldmeyer, "A survey of techniques and challenges in underwater localization," *Ocean Engineering*, vol. 38, no. 14, pp. 1663–1676, 2011.

[6] P. Pandey, M. Hajimirsadeghi, and D. Pompili, "Region of feasibility of interference alignment in underwater sensor networks," *IEEE Journal of Oceanic Engineering*, vol. 39, pp. 189 – 202, 01/2014 2014.

[7] E. Calvo and M. Stojanovic, "Efficient channel-estimation-based multiuser detection for underwater cdma systems," *Oceanic Engineering, IEEE Journal of*, vol. 33, no. 4, pp. 502–512, 2008.

[8] D. Pompili, T. Melodia, and I. F. Akyildiz, "A cdma-based medium access control for underwater acoustic sensor networks," *Wireless Communications, IEEE Transactions on*, vol. 8, no. 4, pp. 1899–1909, 2009.

[9] K. B. Kredo II and P. Mohapatra, "A hybrid medium access control protocol for underwater wireless networks," in *Proceedings of the second workshop on Underwater networks*. ACM, 2007, pp. 33–40.

[10] M. Lotter and P. Van Rooyen, "An overview of space division multiple access techniques in cellular systems," in *Communications and Signal Processing, COMSIG'98. Proceedings of the 1998 South African Symposium on*. IEEE, 1998, pp. 161–164.

[11] M.-O. Pun, V. Koivunen, and H. V. Poor, "Opportunistic scheduling and beamforming schemes for mimo-sdma downlink systems with linear combining," *Submitted to IEEE Journal Select. Areas Commun*, 2007.

[12] S. V. Bana and P. Varaiya, "Space division multiple access (sdma) for robust ad hoc vehicle communication networks," in *Intelligent Transportation Systems, 2001. Proceedings. 2001 IEEE*. IEEE, 2001, pp. 962–967.

[13] G. Marsaglia, "Ratios of normal variables," *Journal of Statistical Software*, vol. 16, no. 4, pp. 1–10, 2006.

[14] G. Casella and R. L. Berger, *Statistical inference*. Duxbury Press Belmont, CA, 2002, vol. 70.

[15] S. J. Orfanidis, *Electromagnetic waves and antennas*. Rutgers University, 2002.

[16] S. S. Rao, *Reliability-based design*. McGraw-Hill Companies, 1992.

[17] J. M. Borwein and A. S. Lewis, *Convex analysis and nonlinear optimization: theory and examples*. Springer, 2010, vol. 3.

[18] Y. Xiao, *Underwater acoustic sensor networks*. CRC Press, 2010.